2019

The Influence of 3D Porous Chitosan-Alginate Biomaterial Scaffold Properties on the Behavior of Breast Cancer Cells

Minh-Chau N. Le
University of Central Florida

THE INFLUENCE OF 3D POROUS CHITOSAN-ALGINATE BIOMATERIAL SCAFFOLD PROPERTIES ON THE BEHAVIOR OF BREAST CANCER CELLS

by

MINH-CHAU N. LE

A thesis submitted in partial fulfillment of the requirements
for the Honors in the Major Program in Mechanical Engineering
in the College of Engineering and Computer Science
and in The Burnett Honors College
at the University of Central Florida
Orlando, Florida

Spring Term 2019

Thesis Co-Chair: Dr. Stephen J. Florczyk
Thesis Co-Chair: Dr. Robert L. Steward

ABSTRACT

The tumor microenvironment plays an important role in regulating cancer cell behavior. The tumor microenvironment describes the cancer cells, and the surrounding endothelial cells, fibroblasts, and mesenchymal stem cells, along with the extracellular matrix (ECM). The tumor microenvironment stiffens as cancer undergoes malignant progression, providing biophysical cues that promote invasive, metastatic cellular behaviors. This project investigated the influence of three dimensional (3D) chitosan-alginate (CA) scaffold stiffness on the morphology, growth, and migration of green fluorescent protein (GFP) – transfected MDA-MB-231 (231-GFP) breast cancer (BCa) cells. The CA scaffolds were produced by the freeze casting method at three concentrations, 2 wt%, 4 wt%, and 6 wt% to provide different stiffness culture substrates. The CA scaffold material properties were characterized using scanning electron microscopy imaging for pore structure and compression testing for Young's Modulus. The BCa cell cultures were characterized at day 1, 3, and 7 timepoints using Alamar Blue assay for cell number, fluorescence imaging for cell morphology, and single-cell tracking for cell migration. Pore size calculations using SEM imaging yielded pore sizes of 253.29 ± 52.45 μm, 209.55 ± 21.46 μm, and 216.83 ± 32.63 μm for 2 wt%, 4 wt%, and 6 wt%, respectively. Compression testing of the CA scaffolds yielded Young's Modulus values of 0.064 ± 0.008 kPa, 2.365 ± 0.32 kPa and 3.30 ± 0.415 kPa for 2 wt%, 4 wt%, and 6 wt% CA scaffolds, respectively. The results showed no significant difference in cell number among the 3D CA scaffold groups. However, the 231-GFP cells cultured in 2 wt% CA scaffolds possessed greater cellular size, area, perimeter, and lower cellular circularity compared to those in 4 wt% and 6 wt% CA scaffolds, suggesting a more prominent presence of cell clusters in softer substrates compared to stiffer substrates. The results also showed cells in 6

wt% CA having a higher average cell migration speed compared to those in 2 wt% and 4 wt% CA scaffolds, indicating a positive relationship between substrate stiffness and cell migration velocity. Findings from this experiment may contribute to the development of enhanced *in vitro* 3D breast tumor models for basic cancer research using 3D porous biomaterial scaffolds.

DEDICATION

For my family, especially my mom, dad, sister, aunts, uncles, and cousins, and Lindsey Webb for their unconditional love and support.

ACKNOWLEDGMENTS

Dr. Stephen J. Florczyk and Dr. Robert L. Steward for their countless hours of support and guidance throughout my undergraduate years.
Zi Wang, Kailei Xu, Isabel Arias, and Sean Beverung for all of the hours teaching and guiding me through the tough times in the lab.

TABLE OF CONTENTS

LIST OF FIGURES

LIST OF TABLES

CHAPTER ONE: INTRODUCTION

Background

Breast cancer (BCa) is the most commonly diagnosed cancer and the second leading cause of death in women. Currently, many pharmaceutical companies utilize two dimensional (2D) culture technologies for drug efficacy and toxicology assessments [1]. However, up to 95% of promising preclinical drugs failed to translate into effective human cancer treatment [2]. One reason for this high rate of failure may be explained by the disparity between the research conducted in 2D cell culture environment and the clinical trials conducted *in vivo* in a three dimensional (3D) environment [3]. The absence of the third dimension in a 2D culture limits the communication between the cancer cells and its tumor microenvironment, affecting cell signaling, vascularization, tumor progression, and metastasis [4]. In recent years, there has been a notable increase in replacing 2D cultures with 3D biomaterials scaffolds for tissue culture in cancer research. 3D scaffolds provide a more physiologically relevant model of the tumor microenvironment compared to 2D surfaces by allowing 3D cell-cell and cell-material interaction that lead to cellular behaviors more closely resembling physiological growth. Particular behaviors include the slower cell growth in 3D cultures that mimic that of cells *in vivo*, and the development of the hollow cores in 3D tumor cultures similar to necrotic areas deprived of nutrients and oxygen in *in vivo* tumors [5]. The effects of scaffold materials on these interactions depend on its mechanical properties such as stiffness, and chemical properties such as composition and presence of proteins [6].

Three Dimensional Biomaterial Scaffolds

In 1988, the term "tissue engineering" (TE) was coined, igniting a new interdisciplinary field that aimed to regenerate damaged tissues by combining cells with 3D porous scaffolds and growth factors [7]. In TE, 3D scaffolds are used as a template that provided the appropriate structural support and environment for cells to adhere and grow, playing the role of a native extracellular matrix (ECM) [7]. As cancer research expanded and the limitations of 2D culture systems were realized, 3D cultures were adapted for use in cancer research, with 3D biomaterial scaffolds being applied as a platform for 3D cultures [2].

Cancer cell morphology and behavior are dominated by the tumor microenvironment [8]. The tumor microenvironment describes the cancer cells, the surrounding endothelial cells, fibroblasts, and the human mesenchymal stem cells that make up the heterogeneous tumor population *in vivo*, and the ECM that serves as the structural support to the cells [9]. Development of 3D cultures is ongoing to create more physiologically relevant 3D breast tumor models, with research on 3D biomaterial scaffold modifications to optimize the growth of BCa cells [6]. These modifications include, but are not limited to, choice of materials (synthetic or natural polymers), porosity, and biochemical factors conjugation [2].

3D culture platforms with tunable mechanical properties must be developed to enable 3D culture systems that may provide valuable *in vivo* predictions. BCa progresses as cells respond to various cues from the microenvironment, changing from a benign phase into a more malignant and invasive state [10]. These biophysical cues from the microenvironment include factors such as the ECM stiffness, pore size, and fiber network [10]. The breast cancer metastatic progression has been observed to occur with the tumor microenvironment transitioning from softer to stiffer tissue.

In a study investigating the elastic moduli of human breast tissue using cylindrical indenter and finite element modelling, breast tissue stiffness ranged from 3.24 ± 0.61 kPa for normal fibrograndular tissue to 42.52 ± 12.47 kPa for high-grade infiltrating ductal carcinoma (IDC) [11].

Breast Cancer Cell Lines

BCa is often classified based on the presence or absence of certain markers to aid in disease prognosis and treatment plan determination. The three most common markers used in classification are estrogen receptor (ER), progesterone receptor (PR), and human epidermal growth factor receptor 2 (HER-2) amplification. An example of a BCa cell line that is ER positive is the MCF-7 cells derived from metastatic pleural effusion of a 69-year-old Caucasian woman [12]. Examples of BCa cell lines that are ER, PR, and HER-2 negative include MDA-MB-468 (468) and MDA-MB-231 (231). 468 cells were derived from metastatic pleural effusion of a 51-year-old Black woman, and 231 cells were derived from metastatic pleural effusion of a 51-year-old Caucasian woman [13].

Breast tumors that lack all three of the molecular markers ER, PR, and HER-2 are called triple-negative breast cancer (TNBC) tumors. TNBC is often diagnosed in female patients under the age of 50, representing between 10% and 24% of BCa cases [14, 15]. TNBC has a high tendency to metastasize and a higher risk for relapse compared to other types of BCa [15]. While tumors that express ER and PR have promising prognosis with therapies that interfere with hormone action or inhibit HER-2 amplification, TNBC tumors have less favorable prognosis due to the lack of the markers [13].

One of the most commonly studied TNBC cell lines is the 231. 231 cells possess a 3D cell morphology of a stellate pattern [16]. A comparison in gene expression between normal breast

cells and tumor cells indicated that 231 cells resemble basal cells on the outside of the breast ducts, categorizing 231 cells as Basal B for molecular classification [13]. With this molecular classification, 231 cell line has a clinical outcome worse than non-basal TNBC cell lines [17].

Cell Morphology in 3D Biomaterial Scaffolds

Cell surface receptors and actin cytoskeleton sense the stiffness of their microenvironment and alter cell morphology and phenotype [5]. In 3D cultures, different subtypes of BCa cells show different growth patterns. For example, 231 cells in 3D cultures show a stellate pattern, while 468 cells possess a grape cluster pattern [13]. When cultured in a 3D environment, BCa cells showed cluster formation, as opposed to those cultured on a 2D surface, which showed a flat shape [18]. More specifically, the 231 2D cell growth has a spindle shape [8]. For 3D cultures in porous poly(ε-caprolactone) (PCL) scaffold with stiffness similar to that of breast tumor tissue, 231 BCa cells formed masses with 3D contact resembling the tumoroids *in vivo* [19].

One of the techniques used to characterize the BCa cell morphology include staining the actin cytoskeleton with Alexa Fluor 546 or 488 Phalloidin, and counterstaining the nuclei with 4,6-diamidino-2-phenylindole (DAPI), then observing the cells using fluorescent microscopy [16, 18, 19]. Another technique is transfecting BCa cells with green fluorescent protein (GFP), which allows GFP-transfected cells to be visualized with a fluorescence microscope [20]. Originally extracted from the jellyfish *Aequorea victoria* in 1992, GFP labeling has been a widely used protein marker.

Cell Growth in 3D Biomaterial Scaffolds

Since cells receive mechanical signals from their environment, it has been shown that scaffold stiffness plays a role in affecting various cellular responses, including cell growth [21]. In

a study investigating the growth of 231 cells on 2D collagen-coupled polyacrylamide gels, it was shown that cells significantly increased in number on the more rigid gels [22]. One possible explanation for the increased 2D gel substrate stiffness leading to increased cell proliferation is that 2D ECM stiffness quickens the cell cycle by influencing the mechanochemical feedback during cell division [23]. However, when proliferation of MCF-7 BCa cells was compared between 3D alginate hydrogels with varied stiffness, the highest cell proliferation characterized by cell cluster formation occurred in the softest 3D hydrogels with stiffness 150 - 200 kPa [18].

In addition to scaffold stiffness, diffusion of nutrients and growth factors also cause differences in proliferation of cells cultured in 2D versus 3D environment [24]. While flat monolayers of cells cultured on 2D surfaces readily receive oxygen and nutrients, spheroids of cells in 3D environment show zones of proliferation due to oxygen and nutrient gradients [5]. Previous research has shown that the growth of tumor cells in 3D scaffolds is usually slower and more closely resembling of the physiological growth than that in 2D surfaces [5].

Migration of Cells Cultured in 3D Biomaterial Scaffolds

Cell migration is a result of force combination involving the actin cytoskeleton, membrane adhesions, and the ECM [25]. In a 3D environment, cell migration is characterized by traction forces exerted by cell-ECM attachments over all surfaces of the cell adhered to the ECM [25]. It has been demonstrated that matrix stiffness influences cell migration in 3D environments since cells can sense the increased ECM stiffness through the transmembrane receptors that bind the cells to their ECM or surrounding cells, and respond with increased traction force on their environment using cytoskeletal networks and molecular motors [10, 26]. In a study investigating how mechanical rigidity of the ECM regulates the behavior of glioma cells using time-lapse

imaging to monitor U373-MG and U87-MG cells over 12 h, it was found that the average migration speed increased with increasing polyacrylamide gel substrate rigidity [23].

There are many techniques to characterize cell migration. One technique is taking time-lapse images of 2D culture samples over a certain time period, and analyzing the images using motion tracking or algorithms in software like SimplePCI [23]. Another is the Boyden Chamber technique, where cells must degrade a collagen barrier to migrate from a non-serum-containing media to a serum-containing media for a specified time period [19]. After this period, migrated cells are stained and counted [19]. A more economical method is the scratch assay that introduces an artificial gap, or scratch, on a confluent cell monolayer. Time-lapse images are captured at the beginning and during the cell migration to close the gap to determine the migration rate [27].

Objectives

The quest for a BCa cure drives the need for improved 3D models that optimize the growth of BCa cells by more accurately mimicking the native tumor microenvironment [6]. As the mechanical properties of the ECM play a critical role in regulating cell behaviors, this research project aims to understand how the mechanical properties of biomaterial scaffolds affect the growth, morphology, and migration of BCa cells. Mechanical properties of the scaffolds, particularly the stiffness, will be changed by preparing chitosan-alginate (CA) scaffolds with different concentrations of chitosan and alginate, with greater concentrations leading to increased stiffness. This study will include 2 wt%, 4 wt%, and 6 wt% 3D porous CA scaffolds. Tissue culture polystyrene (TCPS) well plate will be used as the 2D surface control. In this study, GFP-transfected 231 (231-GFP) BCa cells will be used for cell culture. Since there is currently no

approved targeted therapy for TNBC in clinical settings, a better understanding of the pathogenesis of a TNBC cell line such as 231 is crucial to advancing therapy development [14].

Our hypothesis is that 231-GFP BCa cells cultured on 2 wt% CA scaffolds, with the lowest stiffness, will show the highest cell proliferation. We do not expect differences in morphology among the different groups of 3D porous CA scaffolds. We expect higher cell migration in scaffolds with higher stiffness compared to ones with lower stiffness.

Since cancer progression is often accompanied by changes in cell behavior in response to changes from the tumor microenvironment, understanding how the mechanical properties of CA scaffolds affect the behavior of BCa cells could lead to the development of improved 3D BCa tumor models. Tumor models that more closely depict the dynamic interactions between cancer cells and their microenvironment could potentially enhance the study of disease pathology and development of more effective BCa treatments.

CHAPTER TWO: MATERIALS AND METHODS

Scaffold Fabrication

The 2 wt% CA scaffolds were produced by preparing the 2 wt% alginate and 2 wt% chitosan solutions separately. The 2 wt% alginate solution was prepared by adding alginate to DI water slowly, then soaking for 20 - 30 min before being mixed twice in a Thinky mixer for 3 min at 2000 rpm. The 2 wt% chitosan solution was prepared by adding chitosan to 0.5 wt% acetic acid solution. The chitosan solution was mixed twice in a Thinky mixer for 3 min at 2000 rpm. The alginate and chitosan solutions were aged overnight at room temperature to allow for complete dissolution of the polymers. Then, the alginate and chitosan solutions were mixed together twice in a Thinky mixer for 5 min at 2000 rpm. The mixed CA solution was cast into molds and frozen overnight at -20 °C. The scaffolds were freeze dried for 24 h or until they are dry. The scaffolds were then sectioned into 2 mm thick disks using a razor blade. Next, the scaffolds were crosslinked with 0.2 M $CaCl_2$ solution for 20 min under vacuum. Finally, the scaffolds were sterilized with 70% ethanol under vacuum for 30 min in two 15 min sessions. In between the sessions, the 70% ethanol solution were replaced with fresh 70% ethanol solution. Afterwards, the sterilized scaffolds were washed with Dulbecco's phosphate buffered saline (DPBS) three times in a sterile setting. The 4 and 6 wt% CA scaffolds were prepared with respective increases in chitosan and alginate content, with 1 and 1.5 wt% acetic acid solution used for the chitosan solutions. Table 1 summarizes the components and their amounts used to produce each type of CA scaffold. All sterilized CA scaffolds were soaked in fully supplemented media for 24 h at 37 °C before cell seeding.

Table 1. Components of alginate and chitosan solutions.

	Alginate Solution		**Chitosan Solution**		
Wt %	Alginate	DI Water	Chitosan	Acetic Acid	DI Water
2	2.084	100	2.084	0.5	99.5
4	4.167	100	4.167	1	99
6	6.25	100	6.25	1.5	98.5

Compression Testing

CA scaffold samples were cut to a size of 5 mm x 5 mm x 5 mm. Compression testing was completed using the Shimadzu AGS-X Universal Electromechanical Tester. Wet samples were compressed at a rate of 0.4 mm/min with a 500 N load cell (n = at least 6 per condition). Two types of Young's moduli, or stiffness, were determined from the stress vs. strain plots obtained by the Trapezium X Universal Testing Software as shown in Figure 1. The first type is the bulk stiffness obtained from the slope of the first linear region of the plots, indicating the stiffness associated with compressing the pores of the scaffolds. The second type is the wall stiffness obtained from the slope of the second linear region of the plots, indicating the stiffness associated with the scaffold material after the pores have been compressed [28]. The stiffness values were calculated using the Trapezium X Universal Testing Software.

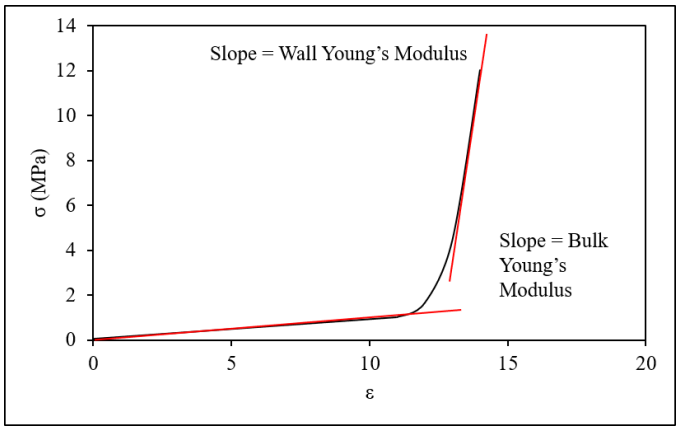

Figure 1. An example of a stress-strain plot obtained from a compression test.

Scanning Electron Microscopy Imaging

CA scaffolds (n = 3 per scaffold type) were imaged on the JEOL JSM-6480 SEM. The scaffold samples were sputter coated with gold prior to imaging. The average pore size (μm) of each CA scaffold type was calculated from the SEM images using the line intercept method adapted from the American Society for Testing and Materials (ASTM) E4 standard for calculating average grain size. Five horizontal lines of equal length were placed at regular intervals over the image and the number of pores the measuring line crossed were counted. The pore size was calculated with the following formula.

$$\text{Pore size } (\mu\text{m}) = \frac{\text{length of measuring line } (\mu\text{m})}{\text{number of pores measuring line crossed}}$$

Cell Seeding on Scaffolds

MDA-MB-231-GFP (231-GFP) BCa cells were cultured and expanded to 80% confluency in T75 cell culture flasks in fully supplemented media (Dulbecco's Modified Eagle's medium (DMEM) with 10% FBS, 1% penicillin-streptomycin, and 1% non-essential amino acids (NEAA)), and incubated at 37 °C prior to cell seeding. 231-GFP BCa cells were detached from T75 cell culture flasks by using Trypsin. Media was aspirated from T75 flasks leaving 231-GFP

cells attached at the bottom surface of the flasks. 3 mL of Trypsin was added to each T75 flask and flasks were incubated at 37 °C for 5 min. 2 mL of fully supplemented media was added to each T75 flask to neutralize Trypsin. The flask surface with cells attached were washed with the neutralized Trypsin solution several times to detach all cells. The neutralized Trypsin-cell solution from each flask was collected in a 50 mL tube, which was centrifuged at 200 g for 10 min to get the cell pellet. The supernatant was aspirated from the 50 mL tube leaving the cell pellet. Cells were resuspended in fully supplemented media and seeded onto 2D surfaces and CA scaffolds in 12-well plates at 50,000 cells per sample. The samples were cultured in fully supplemented media and at 37 °C with 5% CO_2 in a humidified incubator. The samples were cultured for 7 days with regular media changes.

Cell Number Analysis

The growth of BCa cells in 2D cultures and 3D CA scaffolds was assessed with Alamar Blue assay (n = 4 per scaffold type) on day 3 and day 7. Cell culture media in samples was aspirated and samples were washed one time with DPBS. 10% Alamar Blue solution in fresh cell culture media was added to samples and the samples were incubated at 37 °C for 2 h. Alamar Blue solutions was transferred from the samples to a black bottom 96-well plate and read with the BioTek Cytation5 Cell Imaging Multi-Mode Reader at excitation wavelength of 570 nm and fluorescent emission wavelength of 585 nm. The fluorescence results were compared to a standard curve to determine cell population.

Cell Morphology Analysis

The cell morphology of BCa cells cultured on 2D surfaces and 3D CA scaffolds were assessed (n > 50 per scaffold type) on day 1, 3, and 7 timepoints. Samples were fixed with 3.7%

formaldehyde and imaged with the BioTek Cytation5 Cell Imaging Multi-Mode Reader using the GFP filter at excitation wavelength of 490 nm and fluorescent emission wavelength of 510 nm on day 1, 3, and 7 timepoints. Cellular morphology analysis was conducted using BioTek Gen5 Software on day 1, and 3 timepoints. Analysis parameters included circularity, size, area, and perimeter. Circularity was calculated based on an ellipse formula where 1 equals a perfect circle. Size was determined using an ellipse equation fit on the cell contour. Area was calculated based on the number of pixels inside the cell contour. Perimeter was calculated by counting the edge pixels along the cell boundary. Morphology analysis for day 7 cultures was not performed due to the large number of cells in culture leading to noisy GFP signals picked up by the analysis software.

Cell Migration Analysis

BCa cell migration was assessed ($n > 50$ per scaffold type) at day 7 timepoint. Cells cultured on 2D surfaces and 3D scaffolds were harvested by incubating the samples in Accumax solution at room temperature for 15 min. The cells were washed off the scaffolds by pipetting the Accumax solution on the scaffold surface 10 - 20 times. The Accumax solution from each sample group were collected in a 50 mL tube with filled with 7 mL media and centrifuged at 200 g for 10 min to get the cell pellet. The supernatant was aspirated leaving the cell pellet. Cells were resuspended in fully supplemented media, and seeded on glass-bottom Petri dishes filled with fully supplemented media. A cell seeding solution density of 1 million cells/mL was used. A volume of 100 uL of seeding solution was added to each dish to achieve 100,000 cells/dish. Samples are incubated overnight at 37 °C. Samples were rinsed with DPBS one time to remove unattached cells from gels before migration experiment proceeded. 2 mL of fresh fully supplemented media was added into each dish.

Samples were imaged using the ZEISS Cell Observer SD confocal microscope with a motorized scanning stage. Brightfield and fluorescence images were taken at 20× magnification. Time-lapsed images were acquired every 10 min for 3 h. Time-lapsed videos were analyzed and single-cell migration velocity on each sample were determined using MATLAB and Cell Tracker. Briefly, the positions of a cell at each specific timepoint were manually specified by clicking on the centroid of the same cell in the images. The time interval between each image was specified as 10 min. The distance the cell traveled between timepoints was calculated by Cell Tracker using the pixel size. The average cell migration speed for the single tracked cell was calculated by the software.

Statistically Analysis

All data were statistically analyzed and presented as mean ± standard deviation of the mean. A p-value of $p < 0.05$ was set as the statistical significance for all analysis of variance and t-tests.

CHAPTER THREE: RESULTS AND DISCUSSIONS

Scaffold Mechanical Properties

3D porous CA scaffolds were fabricated with varying concentrations to achieve a range of Young's moduli to recapitulate the stiffness changes the native cancer tumor microenvironment issue undergoes throughout cancer progression. The 3D CA scaffolds underwent compression testing in wet condition to better represent the scaffolds state in cell culture media. Compressive testing yielded the bulk and wall Young's moduli, or stiffness, as reported in Figures 2 and 3, respectively. The bulk stiffness of 2 wt%, 4 wt% and 6 wt% CA scaffolds are 2.0 ± 0.1 Pa, 11.7 ± 1.1 Pa and 42.5 ± 0.1 Pa, respectively (Figure 2). The wall stiffness of 2 wt%, 4 wt% and 6 wt% CA scaffolds are 64.0 ± 8.0 Pa, 2.365 ± 0.32 kPa and 3.30 ± 0.415 kPa, respectively (Figure 3). There was significant difference in stiffness among all groups of CA scaffolds. This study focuses primarily on the wall stiffness since it is associated with the scaffold material after the pores have been compressed, indicating the stiffness that the cancer cells sense. The stiffness of normal breast tissue ranges from a fraction of kPa to 3.25 ± 0.91 kPa [11], indicating that the 2 wt%, 4 wt%, and 6 wt% CA scaffolds all have stiffness that fall within the range of normal breast tissue stiffness.

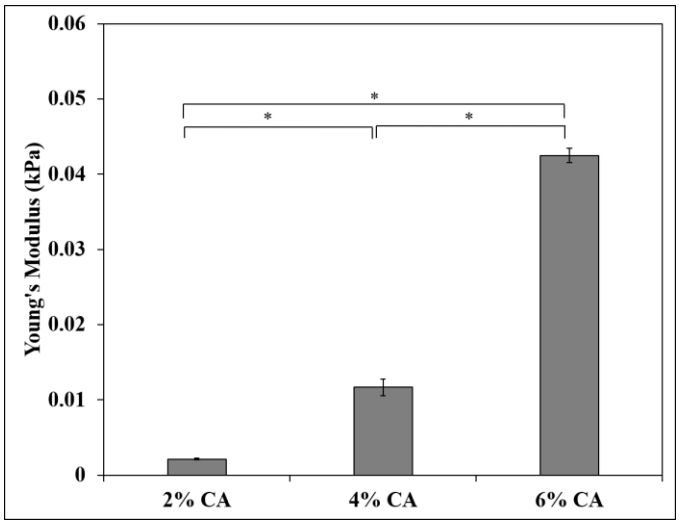

Figure 2. Bulk Young's Modulus of CA scaffolds.

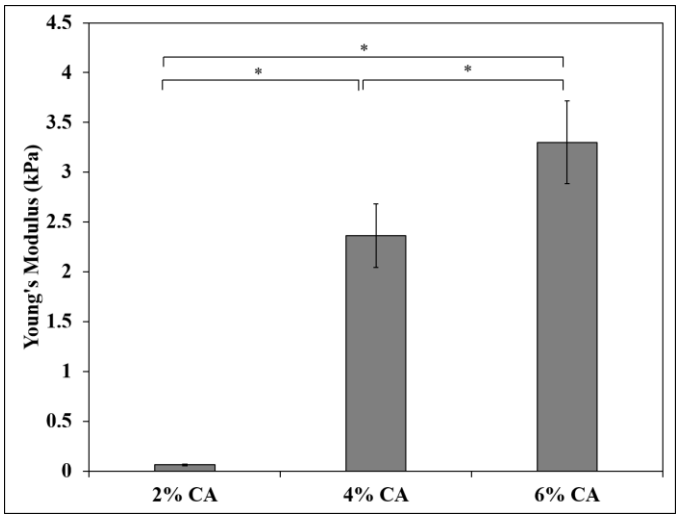

Figure 3. Wall Young's Modulus of CA scaffolds.

In addition to fabricating CA scaffolds with various stiffnesses to simulate the BCa tissue stiffness, scaffolds were also produced using a method that ensured a highly interconnected pore network in the scaffolds as shown in the SEM images in Figure 4. The scaffold fabrication utilized the freeze casting method, where the CA solution was frozen to separate the CA polyelectrolyte complex (PEC) from the solvent, then sublimated, leaving behind the pores that were created by the frozen solvent crystal [29]. The average pore sizes of 2 wt%, 4 wt%, and 6 wt% were calculated

to be 253.29 ± 52.45 µm, 209.55 ± 21.46 µm, and 216.83 ± 32.63 µm, respectively (Figure 5). There is significant difference between the pore sizes of 2 wt% CA scaffolds compared to the rest of the groups. Differences in pore size may be explained by difference in CA solution concentrations since the pore structure of 3D polymer scaffolds depend on several parameters including the concentration of the polymer solution [30].

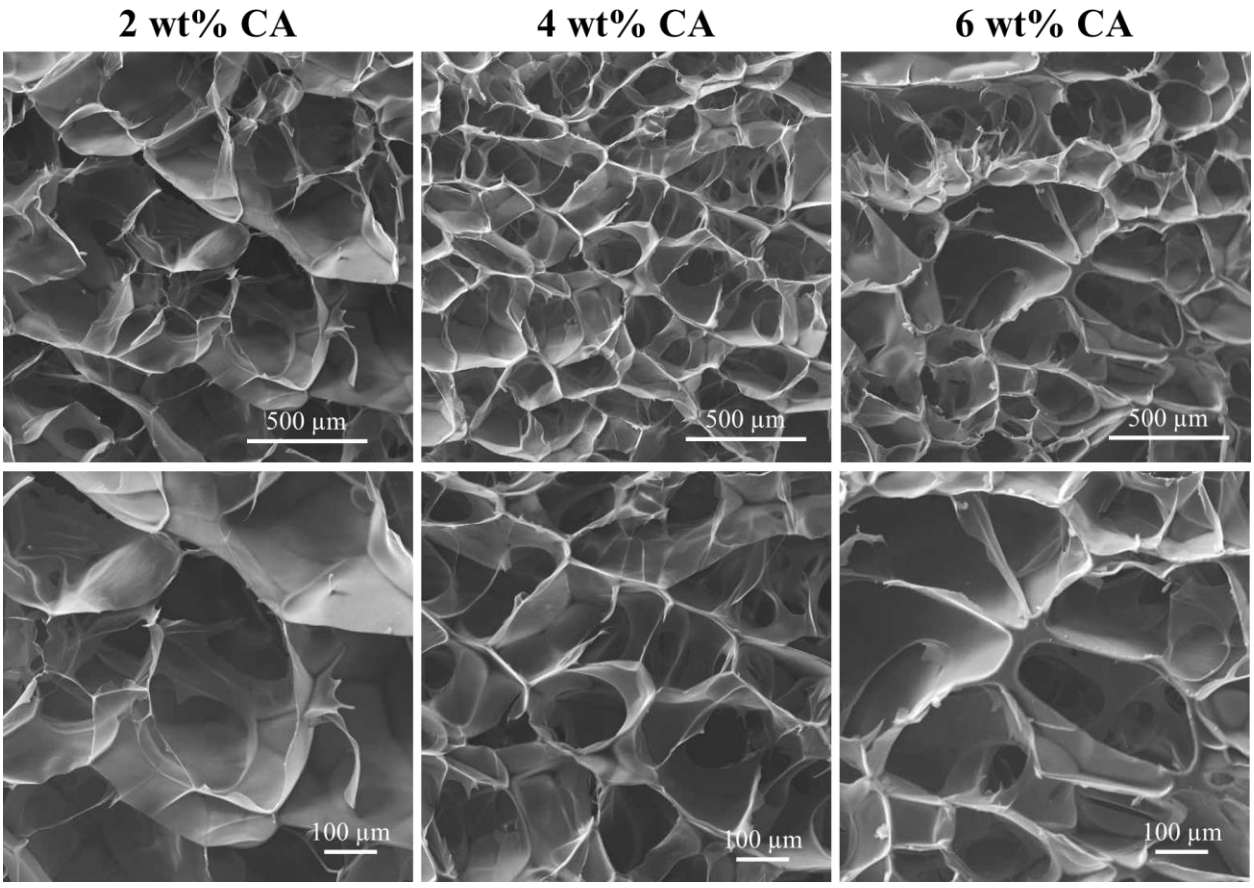

Figure 4. SEM images of the CA scaffolds.

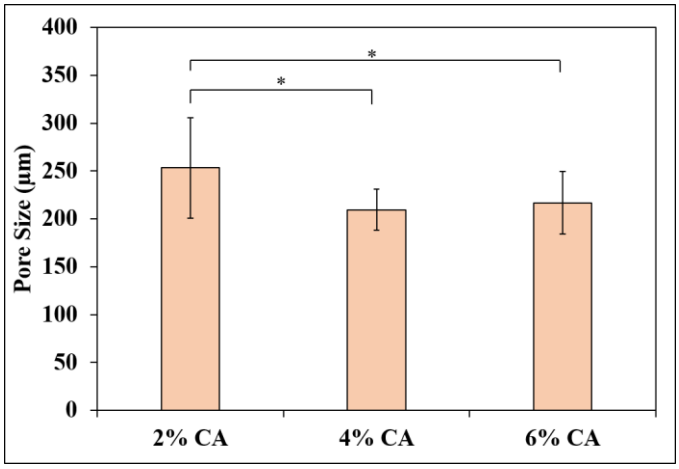

Figure 5. Average pore sizes of the CA scaffolds.

Cell Proliferation

The growth of 231-GFP cells on the scaffolds was characterized at day 3 and day 7 timepoints using Alamar Blue. The CA scaffolds and 2D TCPS control were seeded with 231-GFP and cultured for 7 days with regular media changes. 231-GFP cultured on 3D scaffolds had lower cell numbers compared to those on 2D surfaces on both timepoints (Figure 6). The lower cell number in 3D cultures was expected as cells in a 3D environment experience a limit in nutrients and oxygen diffusion while cells in flat monolayers on 2D surfaces readily receive oxygen and nutrients [5]. However, the absence of significant differences in cell number among the CA scaffold groups at both timepoints was unexpected because the effect of ECM stiffness on cancer cell growth has shown the rigidity-dependence growth of 231 cells with 4-5 fold increase in cell number on stiffer substrates [22]. However, differences in the effect of matrix stiffness on 231 cell proliferation between previous research and this project can be partially explained by the difference in the chemistry of cell culture substrates. While the mentioned research used collagen-coupled polyacrylamide gels, this project used porous CA scaffolds that lacked proteins such as collagen serving as binding sites for cell surface integrins.

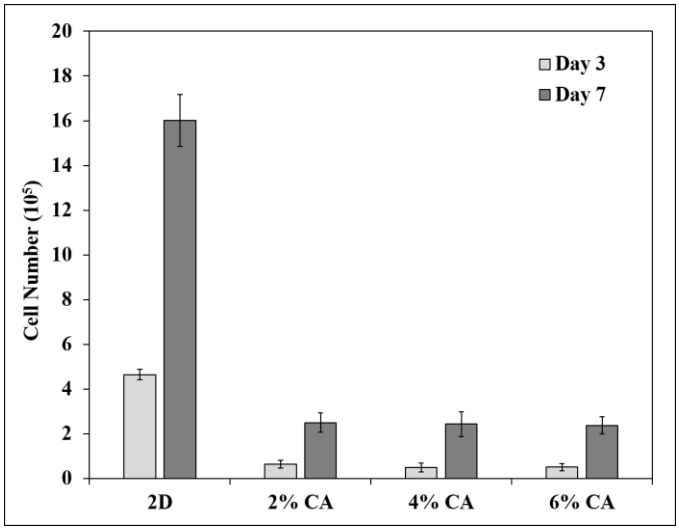

Figure 6. 231-GFP cell number at day 3 and day 7.

Cell Morphology

Fluorescence images of the cell cultures were taken to characterize the effect of ECM stiffness on the morphology of 231-GFP cells at day 1, 3, and 7 timepoints. Figure 7 shows a visual representation of the different cultures on day 1 and day 3. 2D cultures showed a stellate pattern, while cells cultured in 3D scaffolds formed spheroids. This qualitative analysis was supported by the quantification of 231-GFP morphology using cellular circularity. The circularity on day 1 for 231-GFP cells on 2D, 2 wt%, 4 wt%, and 6 wt% CA scaffolds were 0.352 ± 0.213, 0.491 ± 0.234, 0.521 ± 0.244, and 0.544 ± 0.218, respectively. The circularity on day 3 for 231-GFP cells on 2D, 2 wt%, 4 wt%, and 6 wt% CA scaffolds were 0.350 ± 0.209, 0.476 ± 0.238, 0.523 ± 0.245, and 0.532 ± 0.229, respectively. Cells cultured on 2D surfaces possessed significantly lower circularity compared to those cultured in 3D CA scaffolds on both day 1 and day 3 timepoints (Figure 8A). This observation is consistent with a 2015 study investigating the behaviors of 231 cells in 3D porous scaffolds. In this study, 231 cells cultured in 3D porous PCL scaffolds formed tumor-like masses while those on 2D surfaces remained well-spread [19].

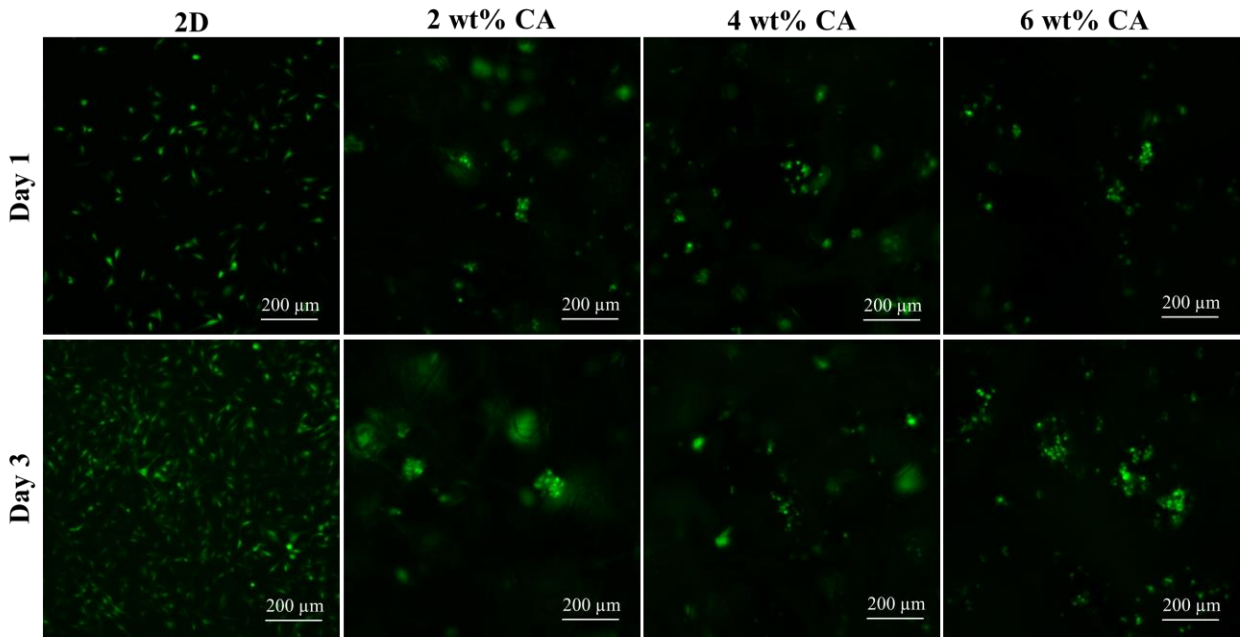

Figure 7. Fluorescence images of the 231-GFP cultures at day 1 and day 3.

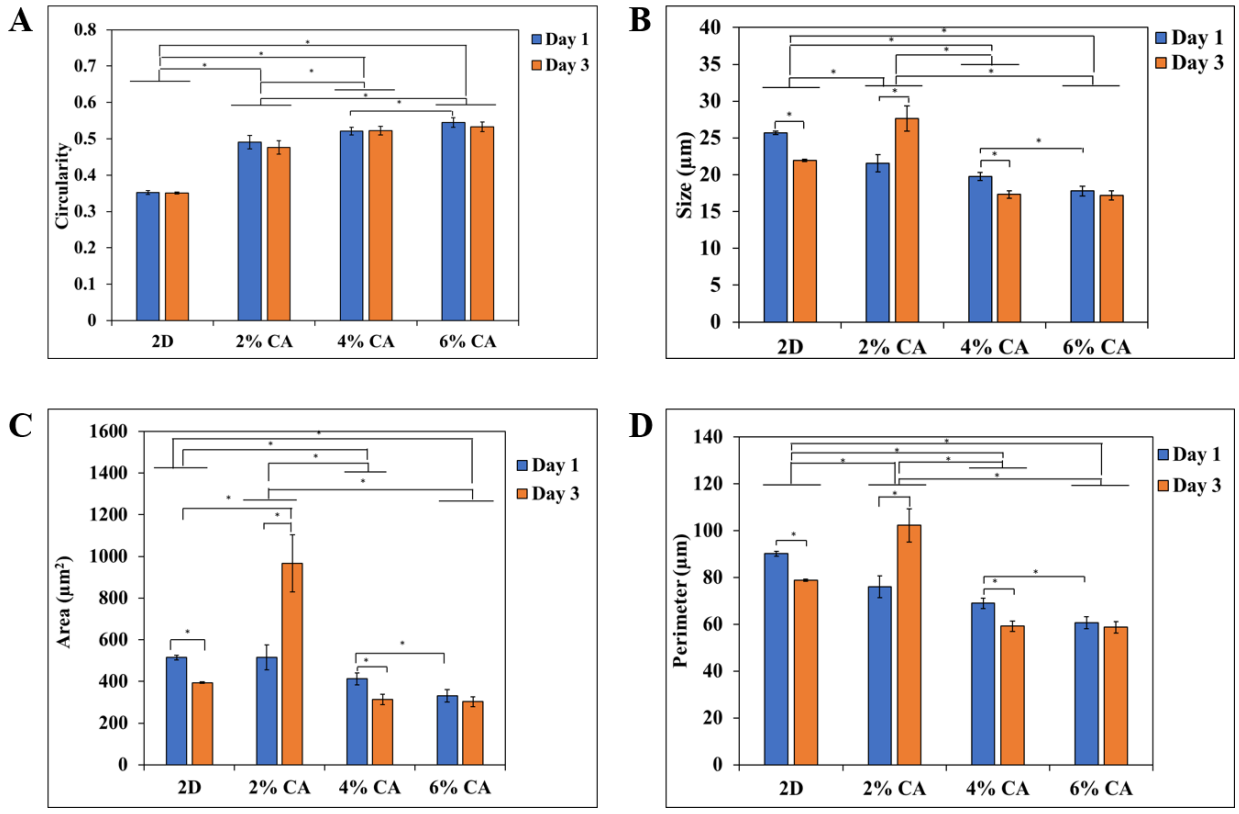

Figure 8. 231-GFP cell morphology characterization at day 3 and day 7. (A) Circularity of 231-GFP cells. (B) Size of 231-GFP cells. (C) Area of 231-GFP cells. (D) Perimeter of 231-GFP cells.

Further quantification of morphology parameters such as size, area, and perimeter was done on day 1 and day 3 (Figures 8B – 8D). 231-GFP cells cultured in 2 wt% CA possessed significantly higher size, area, and perimeter, as compared to those cultured in 4 wt% and 6 wt% CA scaffolds. More specifically, cellular size on day 3 for cells cultured in 2 wt%, 4 wt%, and 6 wt% were 21.952 ± 9.455 µm, 27.645 ± 22.726 µm, 17.322 ± 11.076 µm, and 17.204 ± 10.504 µm, respectively. Based on the size of single 231 cells to be 12.4 ± 2.1 µm in diameter [31], the obtained results on cellular size indicated the presence of more cell clusters in the softest of the CA scaffolds groups. A similar trend in the dependence of the formation of 231 cell clusters on matrix stiffness was shown in a previous study where cells on softer polyacrylamide gel substrates

stayed in clusters due to stronger cell-cell interaction, while those on stiff polyacrylamide gel substrates showed single-cell adhesion due to stronger cell-matrix interaction [32].

The formation of cell clusters also affected cellular circularity of cells cultured on the different 3D porous CA scaffold groups. Figure 8A also shows that cells on 2 wt% CA scaffolds had a lower circularity compared to those on 4 wt% and 6 wt% CA scaffolds. Figure 9 supported this analysis by showing high magnification images on day 7 of 2 wt% CA scaffolds with dense cell clusters forming irregular shapes, hence the lower circularity, compared with 4 wt% and 6 wt% CA scaffolds with smaller clusters and more individual round cells.

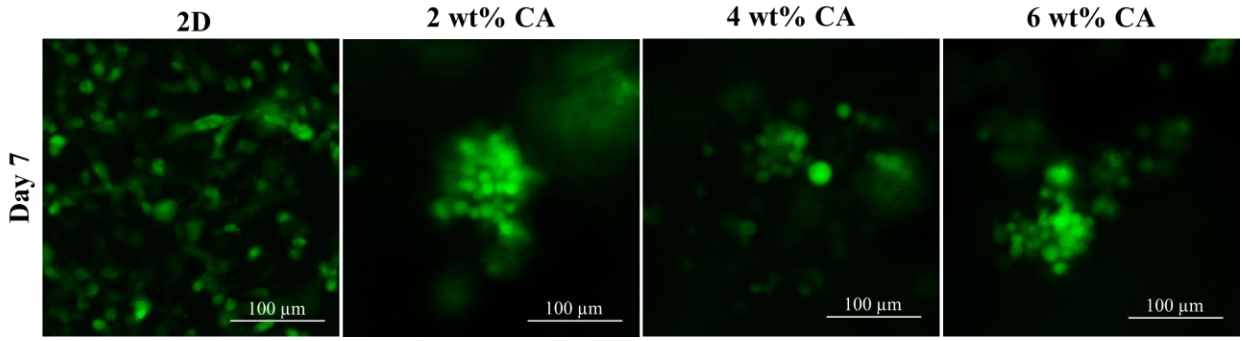

Figure 9. Fluorescence images of the 231-GFP cultures at day 7.

Cell Migration

BCa cell migration speed is closely related to the progression of BCa from a benign state to a more malignant, invasive state due to the stiffening of the ECM. The migration of 231-GFP cells cultured on 3D porous CA scaffolds was analyzed. 231-GFP cells were detached from 3D CA scaffolds and 2D control surfaces on day 7 and seeded onto glass-bottom Petri dishes for the migration experiment. The average migration speed of 231-GFP cells cultured in 3D scaffolds was calculated by tracking single cells for 3 h on time-lapse videos using Cell Tracker on MATLAB. Figure 10 shows an example of this cell tracking process. The red dots show the position of the

tracked cell at a timepoint. The red line connecting the dots together at 3 h estimated the path that the cell traveled. The average cell migration speed was calculated by dividing the distance cell traveled between two timepoints by the amount of time elapsed.

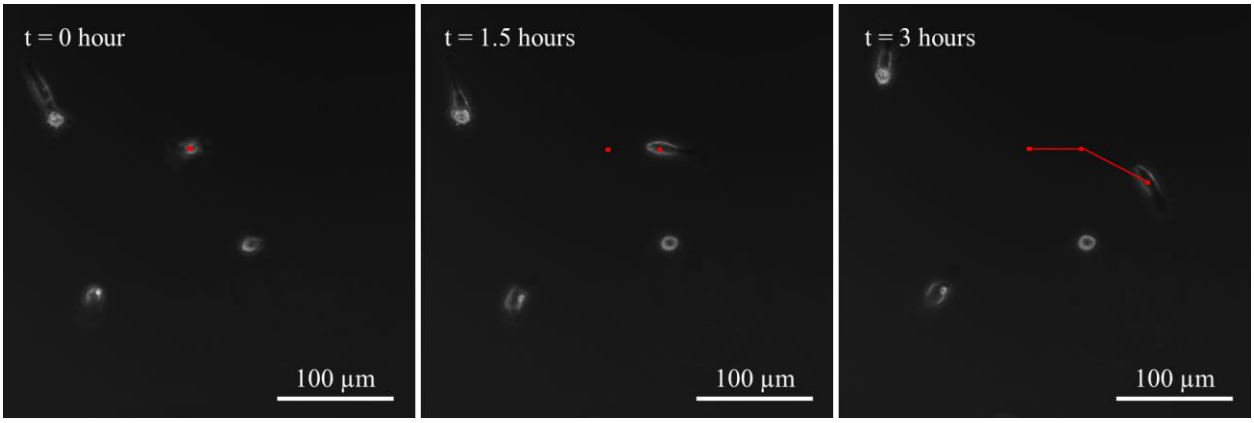

Figure 10. Single-cell tracking for migration speed determination.

The average cell migration speeds for 2D, 2 wt%, 4 wt%, and 6 wt% CA scaffolds were 0.321 ± 0.151 µm/min, 0.291 ± 0.141 µm/min, 0.338 ± 0.115 µm/min, and 0.413 ± 0.143 µm/min, respectively. Significant differences were observed between 6% CA and the remaining of the sample groups as indicated on Figure 11. The literature has shown that cancer cells sense the ECM stiffness and respond by generating traction forces on their surrounding environment [26]. A study done with glioma cells on polyacrylamide gels showed that average migration speeds for U373-MG and U87-MG cells decreased significantly as culture substrate rigidity decreased [23]. While the result of cells in 6 wt% CA scaffold possessing the highest migration speed among the CA scaffold groups due to its stiffness was expected, the absence of difference in migration speed between 2D, 2 wt% CA, and 4 wt% CA scaffolds despite the difference in substrate stiffness was not expected. The lack of difference in cell migration speed between 2D and the 3D groups of 2 wt% and 4 wt% may be explained by the difference in the dimensions of the cell culture format.

The added dimension in 3D culture platform as compared to 2D may have elicited other phenotypic and genotypic cellular responses affecting migration speed that are beyond the scope of pure traction forces. The lack of difference in cell migration speed between the 3D groups of 2 wt% and 4 wt% despite significant difference in stiffness may be due to the observation that their stiffness values both fall within the range for normal breast tissue as found in literature [11].

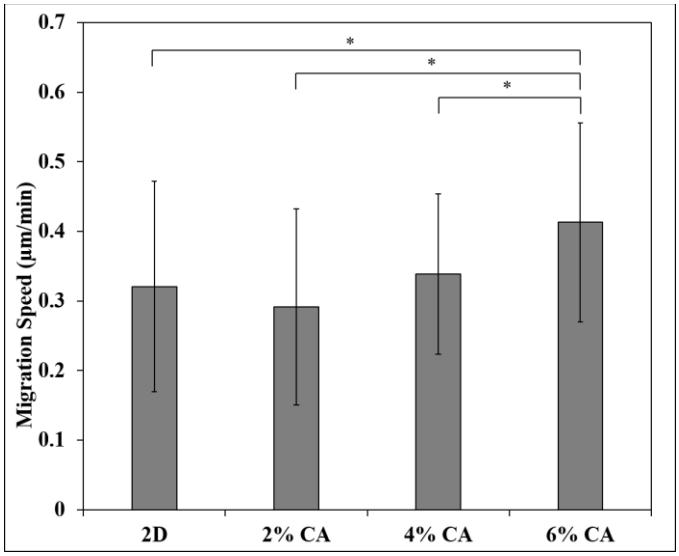

Figure 11. 231-GFP cell migration speed at day 7 timepoint.

CHAPTER FOUR: CONCLUSION AND FUTURE WORK

In conclusion, this project demonstrates the influence of 3D porous CA scaffold stiffness on the behavior of MDA-MB-231 breast cancer cells. The fabricated 2 wt%, 4 wt%, and 6 wt% 3D porous CA scaffolds had stiffness in the range of normal breast tissue and fibrograndular tissue. The results showed increased average migration speed for cells in 6 wt% CA scaffolds compared to those in scaffolds of lesser stiffness, indicating the dependence of 231-GFP migration speed on 3D substrate stiffness. The data also showed lower cellular circularity and higher cell size, area, and perimeter for 231-GFP cultured in 2 wt% CA scaffolds compared to those in scaffolds of higher stiffness, indicating the dependence of 231-GFP migration morphology on 3D substrate stiffness. Findings from this project may contribute to future fabrication of 3D porous scaffolds aiming to mimic the ECM of normal breast tissue and fibroglandular tissue to create a more predictive model of BCa progression with varying ECM stiffness.

As discussed throughout the previous section, there were a few unexpected results such as the lack of difference in cell growth among the 3D scaffold groups, and the lack of difference in cell migration speeds between 231-GFP cells in 2 wt% and 4 wt% CA scaffolds. Some immediate steps that can be taken following this project are further characterizing the proliferation of MDA-MB-231 cells in 3D porous CA scaffolds by culturing cells over a time period longer than 7 days and eliciting significant difference in migration speed by fabricating CA scaffolds with stiffness that span the entire range of breast tissue from normal breast tissue stiffness of less than 1 kPa to invasive IDC stiffness of over 42.52 kPa.

REFERENCES

[1] M. Rimann, U. Graf-Hausner, Synthetic 3D multicellular systems for drug development, Curr Opin Biotechnol 23(5) (2012) 803-9.

[2] P.S. Thakuri, C. Liu, G.D. Luker, H. Tavana, Biomaterials-Based Approaches to Tumor Spheroid and Organoid Modeling, Adv Healthc Mater (2017).

[3] H.B. van der Worp, D.W. Howells, E.S. Sena, M.J. Porritt, S. Rewell, V. O'Collins, M.R. Macleod, Can Animal Models of Disease Reliably Inform Human Studies?, PLoS Med 7(3) (2010).

[4] L.C. Kimlin, G. Casagrande, V.M. Virador, In vitro three-dimensional (3D) models in cancer research: an update, Mol Carcinog 52(3) (2013) 167-82.

[5] D.W. Hutmacher, Biomaterials offer cancer research the third dimension, NATURE MATERIALS 9(2) (2010) 90-93.

[6] G. Rijal, W. Li, 3D scaffolds in breast cancer research, Biomaterials (2016) 135.

[7] F.J. O'Brien, Biomaterials & scaffolds for tissue engineering, Materials Today 14(3) (2011) 88-95.

[8] Z. Liu, G. Vunjak-Novakovic, Modeling tumor microenvironments using custom-designed biomaterial scaffolds, Current Opinion in Chemical Engineering 11 (2016) 94.

[9] A. Villasante, G. Vunjak-Novakovic, Tissue-engineered models of human tumors for cancer research, Expert Opin Drug Discov 10(3) (2015) 257-68.

[10] B. Emon, J. Bauer, Y. Jain, B. Jung, T. Saif, Biophysics of Tumor Microenvironment and Cancer Metastasis - A Mini Review, Comput Struct Biotechnol J 16 (2018) 279-287.

[11] A. Samani, J. Zubovits, D. Plewes, Elastic moduli of normal and pathological human breast tissues: an inversion-technique-based investigation of 169 samples, Phys Med Biol 52(6) (2007) 1565-76.

[12] S. Comsa, A.M. Cimpean, M. Raica, The Story of MCF-7 Breast Cancer Cell Line: 40 years of Experience in Research, Anticancer Res 35(6) (2015) 3147-54.

[13] K.J. Chavez, S.V. Garimella, S. Lipkowitz, Triple negative breast cancer cell lines: one tool in the search for better treatment of triple negative breast cancer, Breast Dis 32(1-2) (2010) 35-48.

[14] A.A. Jitariu, A.M. Cimpean, D. Ribatti, M. Raica, Triple negative breast cancer: the kiss of death, Oncotarget 8(28) (2017) 46652-46662.

[15] Z. Elsawaf, H.P. Sinn, Triple-Negative Breast Cancer: Clinical and Histological Correlations, Breast Care (Basel) 6(4) (2011) 273-278.

[16] P.A. Kenny, G.Y. Lee, C.A. Myers, R.M. Neve, J.R. Semeiks, P.T. Spellman, K. Lorenz, E.H. Lee, M.H. Barcellos-Hoff, O.W. Petersen, J.W. Gray, M.J. Bissell, The morphologies of breast cancer cell lines in three-dimensional assays correlate with their profiles of gene expression, Mol Oncol 1(1) (2007) 84-96.

[17] E.A. Rakha, S.E. Elsheikh, M.A. Aleskandarany, H.O. Habashi, A.R. Green, D.G. Powe, M.E. El-Sayed, A. Benhasouna, J.S. Brunet, L.A. Akslen, A.J. Evans, R. Blamey, J.S. Reis-Filho, W.D. Foulkes, I.O. Ellis, Triple-negative breast cancer: distinguishing between basal and nonbasal subtypes, Clin Cancer Res 15(7) (2009) 2302-10.

[18] M. Cavo, M. Fato, L. Penuela, F. Beltrame, R. Raiteri, S. Scaglione, Microenvironment complexity and matrix stiffness regulate breast cancer cell activity in a 3D in vitro model, Sci Rep 6 (2016) 35367.

[19] G.M. Balachander, S.A. Balaji, A. Rangarajan, K. Chatterjee, Enhanced Metastatic Potential in a 3D Tissue Scaffold toward a Comprehensive in Vitro Model for Breast Cancer Metastasis, ACS Appl Mater Interfaces 7(50) (2015) 27810-22.

[20] S. Raimondo, C. Penna, P. Pagliaro, S. Geuna, Morphological characterization of GFP stably transfected adult mesenchymal bone marrow stem cells, Journal of Anatomy 208(1) (2006) 3-12.

[21] R.G.M. Breuls, T.U. Jiya, T.H. Smit, Scaffold Stiffness Influences Cell Behavior: Opportunities for Skeletal Tissue Engineering, Open Orthop J 2 (2008) 103-9.

[22] R.W. Tilghman, C.R. Cowan, J.D. Mih, Y. Koryakina, D. Gioeli, J.K. Slack-Davis, B.R. Blackman, D.J. Tschumperlin, J.T. Parsons, Matrix rigidity regulates cancer cell growth and cellular phenotype, PLoS One 5(9) (2010) e12905.

[23] T.A. Ulrich, E.M. de Juan Pardo, S. Kumar, The mechanical rigidity of the extracellular matrix regulates the structure, motility, and proliferation of glioma cells, Cancer Res 69(10) (2009) 4167-74.

[24] R. Edmondson, J.J. Broglie, A.F. Adcock, L. Yang, Three-Dimensional Cell Culture Systems and Their Applications in Drug Discovery and Cell-Based Biosensors, Assay Drug Dev Technol 12(4) (2014) 207-18.

[25] M.H. Zaman, L.M. Trapani, A.L. Sieminski, D. Mackellar, H. Gong, R.D. Kamm, A. Wells, D.A. Lauffenburger, P. Matsudaira, Migration of tumor cells in 3D matrices is governed by

matrix stiffness along with cell-matrix adhesion and proteolysis, Proc Natl Acad Sci U S A 103(29) (2006) 10889-94.

[26] M. Kalli, T. Stylianopoulos, Defining the Role of Solid Stress and Matrix Stiffness in Cancer Cell Proliferation and Metastasis, Front Oncol 8 (2018) 55.

[27] C.C. Liang, A.Y. Park, J.L. Guan, In vitro scratch assay: a convenient and inexpensive method for analysis of cell migration in vitro, Nat Protoc 2(2) (2007) 329-33.

[28] L.J. Gibson, B.A. Harley, M.F. Ashby, Cellular Materials in Nature and Medicine, Cambridge University Press 2010.

[29] S. Deville, Freeze-Casting of Porous Biomaterials: Structure, Properties and Opportunities, Materials (Basel). 2010 Mar 17;3(3):1913-27. doi: 10.3390/ma3031913. eCollection 2010 Mar.

[30] S.J. Florczyk, D.J. Kim, D.L. Wood, M. Zhang, Influence of processing parameters on pore structure of 3D porous chitosan-alginate polyelectrolyte complex scaffolds, J Biomed Mater Res A 98(4) (2011) 614-20.

[31] T.N. TruongVo, R.M. Kennedy, H. Chen, A. Chen, A. Berndt, M. Agarwal, L. Zhu, H. Nakshatri, J. Wallace, S. Na, H. Yokota, J.E. Ryu, Microfluidic channel for characterizing normal and breast cancer cells, Journal of Micromechanics and Microengineering 27(3) (2017) 035017.

[32] Y. Wang, T. Gong, Z.R. Zhang, Y. Fu, Matrix Stiffness Differentially Regulates Cellular Uptake Behavior of Nanoparticles in Two Breast Cancer Cell Lines, ACS Appl Mater Interfaces 9(31) (2017) 25915-25928.